Molybdenum complexes of poly[(methylthio)methyl]borates

Ondřej Mrózek [a], Jaromír Vinklárek [a], Libor Dostál [a], Zdeňka Růžičková [a], Jan Honzíček [b,*]

[a] Department of General and Inorganic Chemistry, Faculty of Chemical Technology, University of Pardubice, Studentská 573, 532 10 Pardubice, Czech Republic.

[b] Institute of Chemistry and Technology of Macromolecular Materials, Faculty of Chemical Technology, University of Pardubice, Studentská 573, 532 10 Pardubice, Czech Republic.

[*] Corresponding author. Tel: +420/46603 7229. Fax: +420/46603 7068

E-mail address: jan.honzicek@upce.cz (J. Honzíček)

Keywords: Molybdenum; scorpionates; poly[(methylthio)methyl]borates; NMR spectroscopy; X-ray diffraction.

Highlights:

Coordination modes of two sulfur-donor scorpionate ligands were investigated.

Structures of two allyl molybdenum(II) complexes were determined by X-ray analysis.

New coordination mode of tetrakis[(methylthio)methyl]borate was described.

Abstract:

Organometallic molybdenum compounds bearing poly[(methylthio)methyl]borates, $[(\eta^3\text{-}C_3H_5)Mo(CO)_2(\kappa^3\text{-}PhTt)]$ and $[Bu_4N][\{(\eta^3\text{-}C_3H_5)Mo(CO)_2Cl\}_2(\kappa^2\text{:}\kappa^2\text{-}RTt)]$, where PhTt = phenyltris[(methylthio)methyl]borate and RTt = tetrakis[(methylthio)methyl]borate, have been obtained by ligand exchange reaction from $[(\eta^3\text{-}C_3H_5)Mo(CO)_2(NCMe)_2Cl]$ and appropriate borate. The PhTt ligand provides tridentate face-capping coordination to the central metal while the RTt acts as a bridging ligand and connects two $[(\eta^3\text{-}C_3H_5)Mo(CO)_2Cl]$

monomeric units by unusual $\kappa^2:\kappa^2$-coordination mode. Both compounds were fully characterized by spectroscopic methods and X-ray crystallography.

Graphical Abstract:
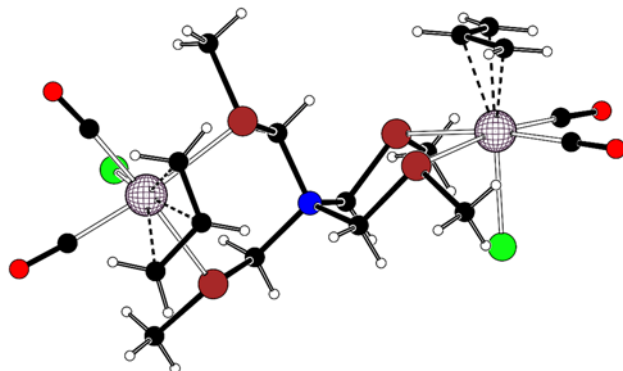
Synopsis:

Molybdenum complexes bearing [(methylthio)methyl]borate ligands were synthesized and characterized by spectroscopic methods. Two structural types were confirmed by X-ray diffraction analysis.

1. Introduction

The discovery of poly(pyrazolyl)borates by Trofimenko *et al.* in 1966 initiated long-standing interest in coordination chemistry of tridentate face-capping ligands [1–6]. Due to the tripodal coordination mode to the metal atoms, the poly(pyrazolyl)borates and their congeners have become known as scorpionates [4]. The main advantage of scorpionate ligands lies in simple modifications of the parent structure that enables a fine tuning of their electronic and steric properties, which is very useful for design of new catalysts [7–10], modelling of active site of metalloenzymes and drug design [11–15].

Scorpionate ligands with sulfur donor atoms [16–23] are of particular interest mainly due to structural analogy with sulfur-rich metalloenzymes (*e.g.* rubredoxins, deazaflavin reducing hydrogenase, $[NiFe_4S_4]$-based CO-dehydrogenase or FeMo nitrogenase cofactor) [24–27]. The tetrakis[(methylthio)methyl]borate (RTt) ligand, as the first representative of the sulfur donor scorpionates, was described in 1994 and face-capping coordination mode was demonstrated on the $[Bu_4N][Mo(\kappa^3\text{-}RTt)(CO)_3]$ complex [16]. Furthermore, the soft scorpionate in the coordination sphere allows molybdenum atom to be protonated using strong acid to afford hydride compound $[Mo(\kappa^3\text{-}RTt)(CO)_3H]$ [16]. Subsequently, chemistry of various

poly[(alkylthio)methyl]borates have been demonstrated on numerous of metal complexes [17–19,28–30]. For example, bridging coordination of phenyltris[(methylthio)methyl]borate (PhTt) was described for homoleptic copper(I) tetramer [Cu(PhTt)]$_4$ [18]. The sterically demanding phenyltris[(*tert*-butylthio)methyl]borate (PhTt^{tBu}) allows to isolate tetrahedral complexes [(κ^3-PhTt^{tBu})NiCl] [19]. Subsequent reaction with MeLi did not yield expected species with Ni–Me bond but unprecedented metallacycle [(κ^2-PhTt^{tBu})Ni(η^2-CH$_2$SBu^t)] [31]. Although donor-acceptor interactions S → M is by far the most common bond between the borate ligand and metals atom, in several cases, an unspecified η^2- or η^6-bond between borate phenyl moiety and metal has been also described [19,32].
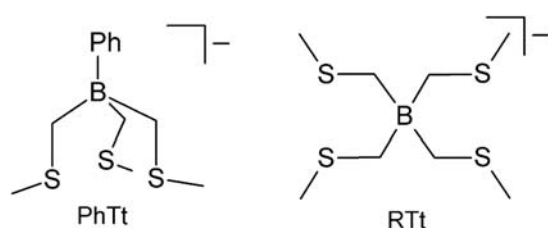

Scheme 1. Ligands used in this work.

The aim of this work is to evaluate coordination properties of two sulphur-donating scorpionate ligands toward molybdenum(II) complex [(η^3-C$_3$H$_5$)Mo(NCMe)$_2$(CO)$_2$Cl] (**1**). Such complex is well-known precursor of scorpionate complexes that enables, in particular case, to isolate κ^2-intermediates as previously demonstrated on reaction with tris(pyrazolyl)methane [33]. In our case, reactivity of typical scorpionate ligand PhTt will be compared with RTt in order to describe the effect of additional (methylthio)methyl function, which could form donor-acceptor interaction with another Lewis acid.

2. Results and discussion

The reaction of [Bu$_4$N][PhTt] with molybdenum(II) complex [(η^3-C$_3$H$_5$)Mo(CO)$_2$(NCMe)$_2$Cl] (**1**) in THF solution gives complex [(η^3-C$_3$H$_5$)Mo(CO)$_2$(κ^3-PhTt)] (**2**), where PhTt acts as a typical tridentate tripodal ligand (Scheme 2). Thus, during the reaction, both acetonitrile ligands as well as chloride are exchanged by three sulfur donor atoms of PhTt.
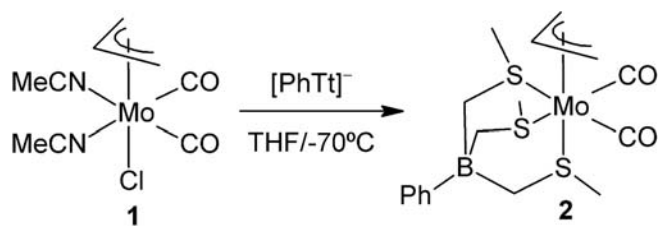
Scheme 2. Syntheses of PhTt complex **2**.

The complex **2** was characterized by multinuclear NMR spectroscopy. ^{1}H and ^{13}C{^{1}H} NMR spectra of **2** reveal one set of signals corresponding with expected C$_s$ symmetry. The low-field signals were assigned to the B–Ph phenyl protons. The allyl ligand gives well-distinguished signals at higher field. In the ^{1}H NMR spectrum, the central proton of the allyl ligand resonates at 4.02 ppm as a triplet of triplet while the dublets at 3.14 ppm ($J = 6.6$ Hz) and 1.51 ppm ($J = 9.9$ Hz) were assigned to *syn-* and *anti*-protons, respectively, based on observed coupling constant values [34]. In ^{13}C{^{1}H} NMR spectrum, allyl carbons resonates at 76.4 (1C) and 57.3 ppm (2C). The methyl and methylene groups of the PhTt ligand appear in ^{1}H NMR spectrum as five broad unresolved resonances with chemical shift in range of 3.0–1.2 ppm. The number of resonances suggests face-capping PhTt coordination mode while their broadness implies fluxional behavior in solution. Since the spectra were measured in non-coordinating solvent, the broadening is hardly caused by some dissociative/associative process. Therefore, it is attributed to a simple conformation change of the metheylene and thiomethyl groups that is in line with literature data published for [(RTt)$_2$Fe] [17].

Table 1. Infrared data for selected η^3-allyl molybdenum complexes.[a]

|	v_a(CO)	v_s(CO)
1	1949 [b]	1851 [b]
2	1945	1860
3	1932	1846
[(η^3-C$_3$H$_5$)(η^5-C$_5$H$_5$)Mo(CO)$_2$]	1963 [c]	1889 [c]

[a] The wavenumber are given in cm^{-1}.
[b] Data reported literature [35].
[c] Data reported literature [36,37].

We note that anionic scorpionate ligands are often taken as more sterically demanding analogues of cyclopentadienyl (Cp) as they donate 6e in face-capping coordination mode. In our case, the formal replacement of Cp by PhTt results in considerably lowering of the carbonyl stretching frequencies (Table 1). It is attributed to diffuse vacant orbitals necessary for π-back bonding, located on thiomethyl functions, leading to limited competition with CO for electron

density. The Cp ligand as well as the PhTt are negatively charged. In case of Cp ligand, the charge is equally distributed over the π-system and contributes to Cp–M bonding. On the contrary, the negative charge of PhTt is formally solely localized on the boron atom with no influence on sulfur–metal bonding situation as unambiguously confirmed by ^{11}B NMR spectroscopy. Hence, the ^{11}B NMR spectrum of **2** shows a sharp signal at −16.8 ppm nearing the value observed for free PhTt anion (−14.4 ppm).[38] This result is in line with previous NMR data obtained for other [(alkylthio)methyl]borate complexes [16,17].
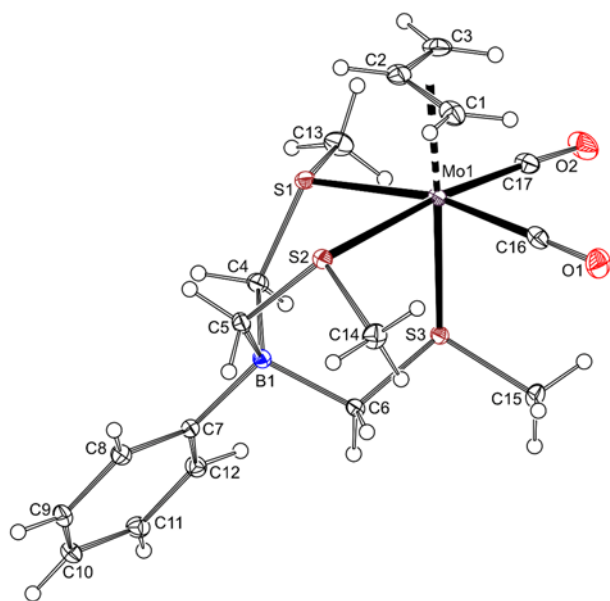
Fig. 1. Molecular structure of $[(\eta^3\text{-}C_3H_5)Mo(CO)_2(\kappa^3\text{-}PhTt)]$ (**2**). Thermal ellipsoids are drawn at the 30% probability level.

Solid-state structure of the compound **2** was determined by single crystal X-ray diffraction analysis (Fig. 1). Selected bond distances and bond angles are listed in Table 2. The molecule **2** shows pseudo-octahedral structure with one face capped by three sulfur donor atoms of PhTt ligand. Remaining three positions are occupied by two carbonyls and centroid of allyl ligand. When the $Cg(\eta^3\text{-allyl})$–Mo bond is taken as a principal axis, sulfur atoms in *trans*-position to carbonyls are considered to lay in equatorial plane (denoted S_{eq}) while the remaining one in axial position (S_{ax}). The framework of the allyl ligand is eclipsed with the OC–Mo–CO moiety, representing the most common arrangement of the $[(\eta^3\text{-}C_3H_5)Mo(CO)_2]$ fragment [39–42]. Due to the *trans*-effect of carbonyl ligands, the bond distances Mo–S_{eq} are considerably shorter than observed for Mo–S_{ax} [ΔMo–S = 0.0871(5) Å]. Similar effect was previously demonstrated on several molybdenum and tungsten complexes [32,42–45]. We note that the Mo–S_{eq} bonds in **2**

are longer than previously reported for molybdenum(0) compound $[Bu_4N][(\kappa^3\text{-}RTt)Mo(CO)_3]$ (Mo–S = 2.571(3), 2.564(3), 2.577(3) Å) [16], which could be related with weaker π-back donation into antibonding σ^*-orbitals of the C–S bonds [47]. Due to steric effect of allyl ligand, the PhTt ligand does not reach typical C_3-symmetrical coordination mode with equal orientation of the methyl groups. As a result, both methyl groups neighboring the allyl ligand are directed below the equatorial plane. This configuration spreads the S–Mo–S bond angle adjacent to thiomethyl groups oriented toward each other [S2–Mo–S3 = 89.03(1) Å].

Table 2. Selected bond lengths (Å) and bond angles (°) of complexes **2** and **3**.

	2	**3**
Mo–S_{eq} [a]	2.5846(5)	2.5937(12); 2.5986(13)
	2.5846(5)	2.6077(12); 2.6052(12)
Mo–X_{ax} [b]	2.4900(5)	2.4853(12); 2.4893(12)
Mo–CO	1.9690(18)	1.964(5); 1.948(5)
	1.9539(17)	1.953(5); 1.953(5)
Mo1–Cg(η^3-allyl) [c]	2.0669(11)	2.040(3); 2.050(3)
S_{eq}–Mo–S_{eq} [a]	80.04(1)	84.67(4); 85.61(4)
S_{eq}–Mo–X_{ax} [a,b]	79.30(1)	84.45(4); 84.72(4)
	89.03(1)	84.36(4); 83.87(4)
CO–Mo–CO	80.28(7)	81.1(2); 79.56(19)
Cg(η^3-allyl) –Mo –X_{ax} [b,c]	174.99(3)	176.75(9); 176.7(9)

[a] S_{eq} is the sulfur atoms in the *trans*-position to carbonyls

[b] X_{ax} is sulfur (for **2**) or chloride (for **3**) atom in the *trans*-position to η^3-allyl

[c] Cg is center of gravity of the allyl

The reaction of **1** with $[Bu_4N][RTt]$ gives dimeric compound $[Bu_4N][\{(\eta^3\text{-}C_3H_5)Mo(CO)_2Cl\}_2(\kappa^2{:}\kappa^2\text{-}RTt)]$ (**3**) in mixture with previously described dimer $[Bu_4N][\{(\eta^3\text{-}C_3H_5)Mo(CO)_2\}_2(\mu_2\text{-}Cl)_3]$ (**4**) [48,49] as evidenced by ^{1}H NMR spectroscopy and mass spectrometry (Scheme 3). Low solubility of **4** in hot hexane enables to isolate the RTt complex **3** in pure form. We note that the yield of **3** strongly depends on reaction conditions. In THF solution, **3** is formed as the main product and was isolated in 55% yield while the use of non-coordinating CH_2Cl_2 produces compound **4** as the only tractable product. We suggest that formation of **3** is in competition previously described solvent-induced ionization of **1**, which

affords $[(\eta^3\text{-}C_3H_5)(CO)_2(NCMe)_3][\{(\eta^3\text{-}C_3H_5)Mo(CO)_2\}_2(\mu_2\text{-}Cl)_3]$ [50]. Due to presence of large ammonium cation, **4** is precipitated as a low soluble species. Analogously, precipitation of $[\{(\eta^3\text{-methallyl})Mo(CO)_2\}_2(\mu_2\text{-}Cl)_3]^-$ anion using Bu_4N^+ has been described recently [23].
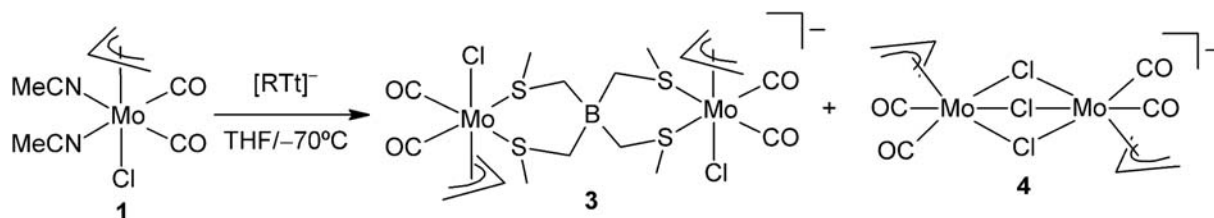

Scheme 3. Reaction of **1** with RTt in THF.

Dimeric nature of the compound **3** was elucidated from mass spectrometry. The base peak in positive mode (m/z = 243) confirms presence of Bu_4N^+ cation while the base peak in negative mode (m/z = 713), with a progression in the isotope pattern by m/z = 1, was assigned to monoanionic species consisting of two $(\eta^3\text{-}C_3H_5)Mo(CO)_2Cl$ moieties and one RTt ligand. Such observation is fully in agreement with ^1H NMR spectrum revealing presence of Bu_4N^+ and η^3-coordinated allyl ligands in molar ratio 1:2. Allyl ligand of the compound **3** gives one triplet of triplets at 3.94 ppm (H^{meso}) and two dublets at 3.08 (H^{syn}) and 1.67 ppm (H^{anti}) in ^1H NMR spectrum and two signals at 74.4 and 57.2 ppm in $^{13}C\{^1H\}$ NMR spectrum implying C_s symmetric coordination sphere of molybdenum. As the dimer **3** belongs to the point group C_2, one may expect appearance of five chemically inequivalent allyl protons and three inequivalent carbons. Different patterns are probably caused by pure delocalization of electron density over the RTt ligand, which results in negligible effects of groups distant from molybdenum that ensures its C_s symmetric coordination sphere. This effect is, of course, further strengthen by fluxional behavior of coordinated RTt ligand. Pure delocalization of negative charge over the borate ligand was, similarly as in the case of **2**, confirmed by ^{11}B NMR spectroscopy. Hence, the dimeric species **3** gives a sharp signal in the same region (−17.9 ppm) as starting $[Bu_4N][RTt]$ (−16.3 ppm). Methyl and methylene protons of coordinated RTt ligand give four broad unresolved signals suggesting twisting of the flexible ligand framework at ambient temperature.

The infrared spectrum of the compound **3** shows two carbonyl stretching bands at ~15 cm^{-1} lower wavenumbers than observed for monomeric species **2** (Table 1). This shift is related with the presence of negatively charged chloride ligand in coordination sphere of molybdenum, which considerably enhances the electron density on the metal.
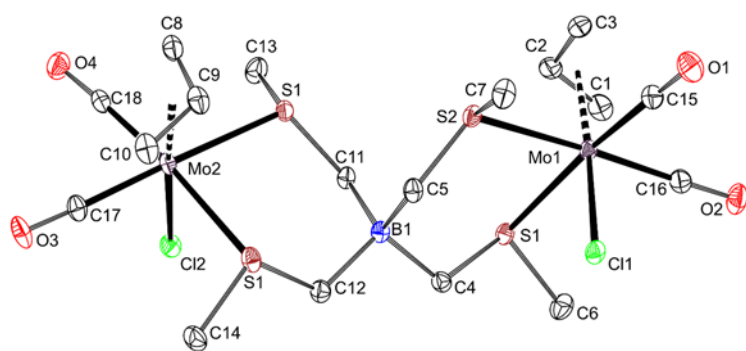
Fig. 2. Molecular structure of $[\{(\eta^3\text{-}C_3H_5)Mo(CO)_2Cl\}_2(\kappa^2{:}\kappa^2\text{-}RTt)]^-$ present in crystal structure of **3**·CH_2Cl_2. Thermal ellipsoids are drawn at the 30% probability level. Hydrogens, Bu_4N^+ cation and CH_2Cl_2 are omitted for clarity.

The solid-state structure of the compound **3** was determined by single crystal X-ray diffraction analysis. It confirms its dimeric nature with two $[(\eta^3\text{-}C_3H_5)Mo(CO)_2Cl]$ units each connected by thiomethyl functions of RTt bridge (Fig. 2). The complex anion has approximate C_2 symmetry arising due to two-fold axis passing through boron atom. Coordination sphere of each molybdenum atom forms distorted octahedron. When the principal axis goes through $Cg(\eta^3\text{-}$allyl)–Mo–Cl moiety, the equatorial plane is occupied with two *cis*-coordinated carbonyl ligands and two sulfur atom of RTt. The framework of the allyl ligand is eclipsed with the moiety OC–Mo–CO moiety similarly as in case of **2**.

The bond lengths Mo–S were found to be significantly longer than observed earlier for Mo–S_{eg} in **2** suggesting stronger *trans*-effect of carbonyl ligands than in case of compound with higher electron density on the molybdenum metal (**3**). Such observation implies stronger Mo–CO bonds, which well correlates with lower CO stretching frequencies mentioned above.

3. Conclusions

In summary, we have evaluated reactivity of $[(\eta^3\text{-}C_3H_5)Mo(CO)_2(NCMe)_2Cl]$ (**1**) toward two sulfur-donor scorpionate ligands (PhTt and RTt). Despite structural similarity, the ligands provide different outcome. The reaction with PhTt gives a compound with well-known face-capping κ^3-coordination mode $[(\eta^3\text{-}C_3H_5)Mo(CO)_2(\kappa^3\text{-}PhTt)]$ (**2**) while additional $MeSCH_2$ arm in RTt enables formation of dimeric species with unprecedented $\kappa^2{:}\kappa^2$-RTt bridge $[\{(\eta^3\text{-}C_3H_5)Mo(CO)_2Cl\}_2(\kappa^2{:}\kappa^2\text{-}RTt)][Bu_4N]$ (**3**). Both organometallic compounds were structurally characterized by X-ray diffraction analysis. Electronic effects of given

[(methylthio)methyl]borate on bonding situation was revealed by multinuclear NMR spectroscopy and infrared spectroscopy.

4. Experimental section

4.1 Methods and Material

All operations were performed under nitrogen using conventional Schlenk-line techniques. The solvents were purified and dried by standard methods [51]. The $[(\eta^3-C_3H_5)Mo(CO)_2(NCMe)_2Cl]$ (**1**), [Bu$_4$N][RTt] and [Bu$_4$N][PhTt] were synthesized according published procedures [16,17,36]. The infrared spectra were recorded in the 4000–400 cm^{-1} region (resolution 1 cm^{-1}) on a Nicolet iS50 FTIR spectrometer using Diamond Smart Orbit ATR. The ^{1}H, ^{13}C{^{1}H} and ^{11}B NMR spectra were measured in CD$_2$Cl$_2$ solutions on a Bruker Avance 500 spectrometer at ambient temperature. NMR chemical shift, given in ppm relative to TMS (^{1}H and ^{13}C{^{1}H}) and BF$_3$·Et$_2$O (^{11}B). The calibration for done on the signal of deuterated solvent (^{13}C{^{1}H}), residual non-deuterated solvent (^{1}H) or external standard B(OMe)$_3$ (^{11}B). Mass spectrometry was performed with a quadruple mass spectrometer (LCMS 2010, Shimadzu, Japan). The sample was injected into the mass spectrometer with infusion mode at a constant flow rate of 10 µL min^{-1}. Electrospray ionization mass spectrometry (ESI-MS) was used for identification of the analyzed samples.

4.2 Synthesis of $[(\eta^3-C_3H_5)Mo(CO)_2(\kappa^3-PhTt)]$ (**2**)

Solution of [Bu$_4$N][PhTt] (1.80 g, 3.50 mmol) in 10 mL of THF was added dropwise *via* cannula to a solution of **1** in 10 mL of THF. The reaction mixture was stirred overnight at room temperature. Then, solvents were vacuum-evaporated and crude complex **2** was washed twice with 8 mL of Et$_2$O. Finally, the compound was recrystallized from a CH$_2$Cl$_2$/hexane mixture to afford yellow crystalline complex **2** (1.02 g, 2.20 mmol, 63 %). Anal. Calc. for C$_{17}$H$_{25}$BMoO$_2$S$_3$: C, 43.97; H, 5.43; S, 20.72. Found: C, 44.18; H, 5.50; S, 20.46%. FTIR (ATR, cm^{-1}): 1945 vs [v$_a$(CO)], 1860 vs [v$_s$(CO)]. ^{1}H NMR (CD$_2$Cl$_2$, 500 MHz, δ ppm): 7.18 (m, 2H, H^{3,5}, C$_6$H$_5$); 7.12 (t, $^3J(^1H,^1H)$ = 7.6 Hz, 2H, H^{2,6}, C$_6$H$_5$); 6.98 (tt, $^3J(^1H,^1H)$ = 7.1Hz, $^4J(^1H,^1H)$ = 1.4Hz, H^4, C$_6$H$_5$); 4.02 (tt, $^3J(^1H,^1H)$ = 9.9 Hz, $^3J(^1H,^1H)$ = 6.6 Hz, H^{meso}, C$_3$H$_5$); 3.14 (d, $^3J(^1H,^1H)$ = 6.6 Hz, 2H, H^{syn}, C$_3$H$_5$); 2.99 (m, 3H, SCH$_3$); 2.39 (m, 6H, SCH$_3$); 2.10 (m, 2H, BCH$_2$); 1.93 (m, 2H, BCH$_2$); 1.59 (m, 2H, BCH$_2$); 1.51 (d, $^3J(^1H,^1H)$ = 9.9 Hz, 2H, H^{anti}, C$_3$H$_5$).

$^{13}C\{^1H\}$ NMR (CD$_2$Cl$_2$, 125.77 MHz, δ ppm): 222.2 (s, 2C, CO); 160.5 (q, $^1J(^{11}B,^{13}C)$ = 51 Hz, 1C, C^1, C_6H_5); 131.4 (s, 2C, C^{3,5}, C_6H_5); 127.6 (s, 2C, C^{2,6}, C_6H_5); 124.5 (s, 1C, C^4, C_6H_5); 76.4 (s, 1C, C^2, C_3H_5); 57.3 (s, 2C, C^{1,3}, C_3H_5); 31.8 (s-br, 3C, PhTt); 28.2 (s-br, 3C, PhTt). $^{11}B\{^1H\}$ NMR (CD$_2$Cl$_2$, 160.42 MHz, δ ppm): −16.8. Single crystals suitable for X-ray analysis were obtain by slow diffusion of hexane into saturated solution of **2** in dichloromethane.

4.3 Synthesis of [Bu$_4$N][{(η^3-C$_3$H$_5$)Mo(CO)$_2$Cl}$_2$(κ^2:κ^2-RTt)] (3)

Solution of [Bu$_4$N][RTt] (1.74 g, 3.50 mmol) in 10 mL of THF was cooled to −80ºC and added dropwise *via* cannula to a solution of **1** in 10 mL of THF precooled to −80ºC. The reaction mixture was allowed to warm to room temperature and the solution was stirred overnight. Then, solvents were vacuum evaporated and crude product was washed twice with 10 mL of hot hexane and 8 mL of Et$_2$O. Finally, the compound was recrystallized from a CH$_2$Cl$_2$/Et$_2$O mixture to afford yellow crystalline complex **3** (1.84 g, 1.93 mmol, 55 %). Anal. Calc. for C$_{34}$H$_{66}$BCl$_2$Mo$_2$NO$_4$S$_4$: C, 40.43; H, 6.59; N, 1.35; S, 12.34. Found: C, 40.73 H, 6.66; N, 1.41; S, 12.63%. FTIR (ATR, cm^{-1}): 1932 vs [ν_a(CO)], 1846 vs [ν_s(CO)]. ^{1}H NMR (CD$_2$Cl$_2$, 500 MHz, δ ppm): 3.94 (tt, $^3J(^1H,^1H)$ = 9.9 Hz, $^3J(^1H,^1H)$ = 6.6 Hz, 2H, H^{meso}, C$_3H_5$); 3.23 (t, $^3J(^1H,^1H)$ = 8.3 Hz, 8H, C^1, Bu$_4$N$^+$); 3.08 (d, $^3J(^1H,^1H)$ = 6.6 Hz, 4H, H^{syn}, C$_3H_5$); 2.23 (s, 4H BCH_2); 2.13 (s, 4H BCH_2); 1.97 (s, 6H, SCH$_3$), 1.67 (m, 8H, C^2, CH_2, Bu$_4$N; 4H,H^{anti}, C$_4H_5$); 1.45 (m, 8H, C^3, CH_2, Bu$_4$N; 4H, BCH_2); 1.02 (t, $^3J(^1H,^1H)$ = 7.3 Hz, 12H, CH_3, Bu$_4$N). $^{13}C\{^1H\}$ NMR (CD$_2$Cl$_2$, 125.77 MHz, δ ppm): 223.6 (s, 2C, CO); 222.1 (s, 2C, CO); 74.4 (s, 2C, C^2, C$_3H_5$); 57.2 (s, 4C, C^{1,3}, C$_3H_5$); 28.0 (s, 2C, RTt); 27.5 (s, 2C, RTt). $^{11}B\{^1H\}$ NMR (CD$_2$Cl$_2$, 160.42 MHz, δ ppm): −17.9. Single crystals suitable for X-ray analysis were obtain by slow diffusion of hexane into saturated solution of **3** in dichloromethane.

4.4 Crystallography

The X-ray data for crystals of **2** and **3**·CH$_2$Cl$_2$ were obtained at 150 K using Oxford Cryostream low-temperature device on a Nonius KappaCCD diffractometer with Mo K$_\alpha$ radiation (λ = 0.71073 Å), a graphite monochromator, and the ϕ and χ scan mode. Data reductions were performed with DENZO-SMN [52]. The absorption was corrected by integration methods [53]. Structures were solved by direct methods (Sir92)[54] and refined by full matrix least-squares based on F^2 (SHELXL97) [55]. Crystallographic data are summarized in Table 3.

Hydrogen atoms were mostly localized on a difference Fourier map, however to ensure uniformity of treatment of crystal, all hydrogen were recalculated into idealized positions (riding model) and assigned temperature factors $H_{iso}(H) = 1.2\ U_{eq}$(pivot atom) or $1.5\ U_{eq}$ for the methyl moiety with C–H = 0.96, 0.93. The thermal ellipsoid of C35 atom in **3**·CH_2Cl_2 was treated with standard ISOR instruction implemented in SHELXL software.

Crystallographic data for structural analysis have been deposited with the Cambridge Crystallographic Data Centre, CCDC nos. CCDC 1818600 and 1818601. Copies of this information may be obtained free of charge from The Director, CCDC, 12 Union Road, Cambridge CB2 1EY, UK (fax: +44-1223-336033; e-mail: deposit@ccdc.cam.ac.uk or www: http://www.ccdc.cam.ac.uk).

Abbreviations

PhTt⁻ = phenyltris[(methylthio)methyl]borate

RTt⁻ = tetrakis[(methylthio)methyl]borate

Acknowledgements

Table 3. Crystallographic data of molybdenum and tungsten compounds.

	2	**3·CH$_2$Cl$_2$**
formula	C$_{17}$H$_{25}$BMoO$_2$S$_3$	C$_{18}$H$_{30}$BCl$_2$Mo$_2$O$_4$S$_4$, C$_{16}$H$_{36}$N, CH$_2$Cl$_2$
cryst. syst.	triclinic	Monoclinic
space group	$P\bar{1}$ (No. 2)	$P2_1/c$ (No. 14)
a (Å)	7.5230(4)	16.4660(9)
b (Å)	10.9771(6)	13.8120(11)
c (Å)	12.2130(4)	23.0971(18)
α (°)	94.043(3)	90
β (°)	101.029(3)	114.144(5)
γ (°)	90.055(4)	90
Z	2	4
μ (mm^{-1})	0.988	0.955
D_x (g cm^{-3})	1.562	1.441
cryst size (mm)	0.28 × 0.31 × 0.56	0.14 × 0.22 × 0.23
cryst color	yellow	yellow
cryst shape	block	block
θ range (°)	3.305–27.500	1.000–27.500
$h\ k\ l$ range	–9/9, –14/14, –15/15	–21/21, –17/17, –30/29
no. of reflns measd	18551	74093
no. of unique reflns; R_{int}[a]	4500; 0.026	10922; 0.068
no. of obsd reflns [$I>2\sigma(I)$]	4275	8597
no. of params	217	460
S[b] all data	1.133	1.173
final R indicies [$I>2\sigma(I)$][c]	R$_1$ = 0.0200 wR$_2$ = 0.0512	R$_1$ = 0.0551 wR$_2$ = 0.1011
fianl R indicies (all data)[c]	R$_1$ =0.0220 wR$_2$ = 0.0527	R$_1$ = 0.0781 wR$_2$ = 0.1149
$\Delta\rho$, max., min. (eÅ^{-3})	0.584, –0.638	1.896, –1.292

[a] $R_{int} = \Sigma|F_o^2 - F_{o,mean}^2|/\Sigma F_o^2$.

[b] $S = \sqrt{\Sigma[w(F_o^2 - F_c^2)^2]/(N_{diffrs} - N_{params})}$.

[c] $R_1 = \Sigma||F_o| - |F_c||/\Sigma|F_o|$, $wR_2 = \sqrt{\Sigma[w(F_o^2 - F_c^2)^2]/\Sigma[w(F_o^2)^2]}$.

References

[1]   J.P. Jesson, S. Trofimenko, D.R. Eaton, J. Am. Chem. Soc. 89 (1967) 3148.

[2]   S. Trofimenko, Chem. Rev. 93 (1993) 943.

[3]   S. Trofimenko, J. Am. Chem. Soc. 88 (1966) 1842.

[4]   S. Trofimenko, Imperial College Press, London, 1999.

[5]   S. Trofimenko, J. Am. Chem. Soc. 92 (1970) 5118.

[6]   M. Pellei, C. Santini, M. Marinelli, A. Trasatti, H.V.R. Dias, Polyhedron 125 (2017) 86.

[7]   P. Neves, S. Gago, S.S. Balula, A.D. Lopes, A.A. Valente, L. Cunha-Silva, F.A.A. Paz, M. Pillinger, J. Rocha, C.M. Silva, I.S. Gonçalves, Inorg. Chem. 50 (2011) 3490.

[8]   M.L. Martins, Catalysts 7 (2017).

[9]   P.A. Ribeiro, A.I. Matias, C.E. Alegria, M.A. Ferraria, M.A. Botelho do Rego, J.A. Pombeiro, M.L. Martins, Catalysts 8 (2018).

[10]   T.F.S. Silva, E.C.B.A. Alegria, L.M.D.R.S. Martins, A.J.L. Pombeiro, Adv. Synth. Catal. 350 (2008) 706.

[11]   C.G. Young, Eur. J. Inorg. Chem. 2016 (2016) 2357.

[12]   C.J. Carrano, Eur. J. Inorg. Chem. 2016 (2016) 2377.

[13]   F. Silva, C. Fernandes, M.P.C. Campello, A. Paulo, Polyhedron 125 (2017) 186.

[14]   P. Smoleński, C. Pettinari, F. Marchetti, M.F.C. Guedes da Silva, G. Lupidi, G.V. Badillo Patzmay, D. Petrelli, L.A. Vitali, A.J.L. Pombeiro, Inorg. Chem. 54 (2015) 434.

[15]   A. V Artem'ev, J.A. Eremina, E. V Lider, O. V Antonova, E. V Vorontsova, I.Y. Bagryanskaya, Polyhedron 138 (2017) 218.

[16]   P. Ge, B.S. Haggerty, A.L. Rheingold, C.G. Riordan, J. Am. Chem. Soc. 116 (1994) 8406.

[17]   C. Ohrenberg, P. Ge, P. Schebler, C.G. Riordan, G.P.A. Yap, A.L. Rheingold, Inorg. Chem. 35 (1996) 749.

[18]   C. Ohrenberg, M.M. Saleem, C.G. Riordan, G.P.A. Yap, A.K. Verma, A.L. Rheingold, Chem. Commun. (1996) 1081.

[19]   P.J. Schebler, C.G. Riordan, I.A. Guzei, A.L. Rheingold, Inorg. Chem. 37 (1998) 4754.

[20]   H.W. Yim, L.M. Tran, E.D. Dobbin, D. Rabinovich, L.M. Liable-Sands, C.D. Incarvito, K.-C. Lam, A.L. Rheingold, Inorg. Chem. 38 (1999) 2211.

[21]   M. Garner, M.-A. Lehmann, J. Reglinski, M.D. Spicer, Organometallics. 20 (2001) 5233.

[22]   M. Garner, J. Reglinski, I. Cassidy, M.D. Spicer, A.R. Kennedy, Chem. Commun. (1996) 1975.

[23]   D. Morales, M. Puerto, I. del Río, J. Pérez, R. López, Chem. Eur. J. 18 (2012) 16186.

[24]   P.A. Lindahl, N. Kojima, R.P. Hausinger, J.A. Fox, B.K. Teo, C.T. Walsh, W.H. Orme-Johnson, J. Am. Chem. Soc. 106 (1984) 3062.

[25]   S.L. Tan, J.A. Fox, N. Kojima, C.T. Walsh, W.H. Orme-Johnson, J. Am. Chem. Soc. 106 (1984) 3064.

[26]   J.-H. Jeoung, H. Dobbek, Science 318 (2007) 1461.

[27]   O. Einsle, F.A. Tezcan, S.L.A. Andrade, B. Schmid, M. Yoshida, J.B. Howard, D.C. Rees, Science 297 (2002) 1696.

[28]   S.-J. Chiou, J. Innocent, C.G. Riordan, K.-C. Lam, L. Liable-Sands, A.L. Rheingold, Inorg. Chem. 39 (2000) 4347.

[29]   M.T. Mock, C. V Popescu, G.P.A. Yap, W.G. Dougherty, C.G. Riordan, Inorg. Chem. 47 (2008) 1889.

[30]   C.G. Riordan, Coord. Chem. Rev. 254 (2010) 1815.

[31]   P.J. Schebler, B.S. Mandimutsira, C.G. Riordan, L.M. Liable-Sands, C.D. Incarvito,

A.L. Rheingold, J. Am. Chem. Soc. 123 (2001) 331.

[32] C. Ohrenberg, C.G. Riordan, L. Liable-Sands, A.L. Rheingold, Coord. Chem. Rev. 174 (1998) 301.

[33] I. Honzíčková, J. Honzíček, J. Vinklárek, Z. Padělková, Polyhedron. 81 (2014) 364.

[34] Y.D. Ward, L.A. Villanueva, G.D. Allred, S.C. Payne, M.A. Semones, L.S. Liebeskind, Organometallics 14 (1995) 4132.

[35] J.C. Alonso, P. Neves, M.J. Pires da Silva, S. Quintal, P.D. Vaz, C. Silva, A.A. Valente, P. Ferreira, M.J. Calhorda, V. Félix, M.G.B. Drew, Organometallics 26 (2007) 5548.

[36] J.W. Faller, C.-C. Chen, M.J. Mattina, A. Jakubowski, J. Organomet. Chem. 52 (1973) 361.

[37] J.W. Faller, D.F. Chodosh, D. Katahira, J. Organomet. Chem. 187 (1980) 227.

[38] J. Tillmann, H.-W. Lerner, M. Bolte, Acta Crystallogr. Sect. E. 66 (2010) o203.

[39] M.J. Calhorda, P.J. Costa, Coord. Chem. Rev. 344 (2017) 83.

[40] D.E. Ryan, D.J. Cardin, F. Hartl, Coord. Chem. Rev. 335 (2017) 103.

[41] L.A. Villanueva, Y.D. Ward, R. Lachicotte, L.S. Liebeskind, Organometallics 15 (1996) 4190.

[42] J.. Ascenso, C.. de Azevedo, M.. Calhorda, M.A.A.. de C.T. Carrondo, P. Costa, A.. Dias, M.G.. Drew, V. Félix, A.. Galvão, C.. Romão, J. Organomet. Chem. 632 (2001) 197.

[43] O. Mrózek, J. Vinklárek, Z. Růžičková, J. Honzíček, Eur. J. Inorg. Chem. 2016 (2016) 5250.

[44] J. Honzíček, J. Vinklárek, M. Erben, J. Lodinský, L. Dostál, Z. Padělková, Organometallics 32 (2013) 3502.

[45] J. Honzíček, P. Kratochvíl, J. Vinklárek, A. Eisner, Z. Padělková, Organometallics 31 (2012) 2193.

[46] J. Honzíček, I. Honzíčková, J. Vinklárek, Z. Růžičková, J. Organomet. Chem. 772–773 (2014) 299.

[47] A. Magistrato, P. Maurer, T. Fässler, U. Rothlisberger, J. Phys. Chem. A. 108 (2004) 2008.

[48] P. Pinto, E. Barranco, M.J. Calhorda, V. Félix, M.G.B. Drew, J. Organomet. Chem. 601 (2000) 34.

[49] J. Perez, D. Morales, V. Riera, A. Rodriguez, S. Garcia-Granda, Dalt. Trans. (2003) 1641.

[50] B.J. Brisdon, M. Cartwright, J. Organomet. Chem. 128 (1977) C15.

[51] W.L.F. Armarego, D.D. Perin, Purification of laboratory chemicals , Butterworth Heinemann, Oxford, Boston, 1996.

[52] Z. Otwinowski, W. Minor, Methods Enzymol. 276 (1997) 307.

[53] P. Coppens, in: F.R. Ahmed, S.R. Hall, C.P. Huber (Eds.), Crystallogr. Comput. Munksgaard, Copenhagen, 1970: p. 255.

[54] A. Altomare, G. Cascarano, C. Giacovazzo, A. Guagliardi, M.C. Burla, G. Polidori, M. Camalli, J. Appl. Crystallogr. 27 (1994) 435.

[55] G.M. Sheldrick, SHELXL97, Univerzity of Göttingen, Germany, 1997.